Green synthesis of copper oxide nanoparticles using Prickly Pear peel fruit extract: characterization and catalytic activity

Abdessalem Badri,[a*] Sami Slimi,[b,c] Mouhieddine Guergueb,[d] Hamza Kahri,[a] Xavier Mateos[b].

[a]*Laboratory of Interfacial and Advanced Materials, Faculty of Sciences, University of Monastir, 5000 Monastir, Tunisia*

[b]*Universitat Rovira i Virgili (URV), Física i Cristal·lografia de Materials i Nanomaterials (FiCMA-FiCNA), Marcel.li Domingo 1, 43007 Tarragona, Spain.*

[c]*I.P.E.I. of Monastir, Unit of Materials and Organic Synthesis, 5019 Monastir, UR17ES31, Tunisia*

[d]*University of Monastir, Laboratoire de Physico-chimie des Matériaux, Faculté des Sciences de Monastir, Avenue de l'environnement, 5019 Monastir, Tunisia*

* Corresponding author: badri_abdessalem@yahoo.fr

Address: Laboratory of Interfacial and Advanced Materials, Faculty of Sciences, University of Monastir, 5000 Monastir, Tunisia. Tel: (216) 73 500 280. Fax: (216) 73 500 278

Abstract

In this work, a rapid and green synthesis of copper oxide nanoparticles was developed using aqueous extract of prickly pear peel. The obtained CuO nanoparticles were characterized by X-ray diffraction (XRD), Fourier transform infrared (FTIR) spectroscopy, transmission electron microscopy (TEM), scanning electron microscopy (SEM) and energy-dispersive X-ray analysis (EDX). The XRD result showed that CuO nanoparticles crystallize in the C 2/c monoclinic space group and confirmed their purity by refinement of the pattern. The FTIR measurements indicated that different phytochemicals present in prickly pear peels extract were responsible for the synthesis of CuO nanoparticles. The UV-visible analysis reported the surface Plasmon resonance band at 284 nm. The SEM and TEM analysis also confirmed that the synthesized nanoparticles had spherical morphology with uniform symmetry and displayed a particle in a 20−40 nm range size. The EDX spectrum and mapping proved the purity of CuO with Cu and O occurrence. Afterward, the catalytic activity of the synthesized catalyst was tested for the reduction of 4-nitrophenol (4-NP) in the presence of sodium borohydride in an aqueous media. Moreover, the catalyst showed high durability during several cycles.

Keywords: Green synthesis, prickly pear, nanoparticles, copper, reduction.

1. Introduction

The field of nanomaterials such as metallic nanoparticles, carbon nanotubes, etc. reveals unique electronic, magnetic, optical, catalytic and medicinal properties compared to ordinary materials due to their large surface to volume ratio, and their high surface energy. Among the different nanomaterials, researchers in nanotechnology pay special attention to copper oxide nanoparticles (CuO-NPs) because of their wide range of applications in catalysis [1-2], photo-catalysis [3-4], optics [5-6], antimicrobial agent [7-9] and biosensors [10-11]. Thus, the biosynthesis of CuO-NPs by green methodologies, being pure and ecological, has been widely used to replace traditional methods of synthesis, such as solid-state reaction [12], sono-chemical [13], rapid precipitation [14], sol-gel technique [15], etc. The advantage of a green method is to minimize the use of hazardous organic solvents, toxic reagents, non-biodegradable stabilizing agents, expensive instruments and the tedious control of the chemical reduction process, as well as to be environmentally friendly. In addition, several plants and plants-based materials are evaluated as a substrate for the synthesis of metallic oxide nanoparticles due to their reduction potentiality and simple scale-up process. Among them, Cactus pear (*Opuntia focus-indica*) is grouped under the *Cactaceae* family. Cactus pear wastages can be very well harnessed and it is one of the most important productive plants per unit of a cultivated field. Its fruit, called prickly pear, has been presented to be a good producer of nutrients and antioxidants [16], and it has healthy benefits such as protective effects of the cardiovascular system, chemopreventive, antiproliferative and anticancer [17]. Further, the green synthesis of nanoparticle using prickly pear aqueous extract showed diverse applications. The fabricated ZnO-NPs by Ethiopian cactus pear fruit peel infusions exhibited greater photocatalytic degradation efficiency of Bisphenol-A (BPA) in water under sunlight irradiation. After 5 repeatable cycles, > 90 % BPA was removed [18]. Furthermore, the activity of Ag-NPs was valued in water from the effluent. So, the growth of coliform bacteria E. coli var 1, E. aerogenes var 1, C. freundii var 2, an atypical E. coli, and aerobic mesophyll microorganisms present in treated wastewater was inhibited with 0.5 mg/ml of Ag-NPs for 0.5 h [19].

In this paper, we demonstrate a novel biological route for the synthesis of CuO-NPs using aqueous extract of prickly pear peels. The use of XRD, FTIR, EDX, SEM, TEM allowed the characterization of the biosynthesized CuO-NPs. The catalytic activity of the biosynthesized CuO-NPs has also been investigated by reduction of 4-nitrophenol (4-NP) to 4-aminophenos (4-AP). The increasing of the experimental temperature was examined and the reutilization of the catalyst was evaluated.

2. Materials and methods

2.1.Reagents

All reagents used in this work are purchased from Sigma Aldrich without purification: copper sulfate pentahydrate ($CuSO_4.5H_2O$, 99%), Sodium borohydride ($NaBH_4$, 98%) and 4-nitrophenol ($C_6H_5NO_3$, 99%). The fresh leaves of prickly pear were collected in Monastir, Tunisia. Double distilled water was used for preparing the solutions.

2.2. Collection of Prickly pear leaf extract

Fresh Prickly pear were collected, washed several times with distilled water and dried. The dried peels were cut into small pieces, finely ground. We weighted 10 g, added them to 100 mL of double-distilled water and stirred at room-temperature for 12h. The reddish extracted solution with pH=6.5 was filtered through Whatman No.1 filter paper thrice to get a clear extract. Then, the collected filtrate was kept at 4 °C and used for further experimental process.

2.3. Synthesis of CuO-NPs

For the green synthesis of CuO using peel prickly pear extract, the latter was used as a chelating agent and copper sulfate pentahydrate as a precursor. In order to prepare 0.1 M solution, we used 100 mL of distilled water to dissolve 2.54 g of copper sulfate pentahydrate while continuously stirring at 150 rpm for 2 h to form a complete homogeneous solution. The obtained solution was was added drop wise using a burette, to the aqueous extract of prickly pear and stirring continuously at 80°C for 2h, until the color of the solution changed into dark brown. This change in color prompted the reduction of copper to form copper oxide. A centrifuge set at 4000 rpm for 15 min was used to remove the biologic compounds attached to the metal nanoparticles. After washing three times with water and two times with ethanol the formed nanoparticles were kept in the oven for aging at 50°C for 12 h. The well-dried copper oxide nanoparticles were hardened at 500°C for 2 h and were tightly bottled for further analysis.

2.4.Characterization of CuO-NPs

The crystalline structure was determined by means of a X-ray diffractometer (XRD) (Philips X'Pert automated diffractometer) with Cu Kα radiation over the range of 2θ=10–80°. Fourier transform infrared (FTIR) spectra of the sample were analyzed using a Perkin Elmer Paragon 1000 PC Fourier Spectrometer in the range of wave number 400–4000 cm^{-1}. Elementary composition, particle dispersion and morphology were examined with a Scanning Electron Microscope with energy dispersive X-ray analysis (SEM-EDX) using a Zeiss evo18 scanning electron microscope. Size, shape and particle distribution were analyzed by transmission electron microscopy (TEM) analysis with a JEOL JEM 2100 microscopy. The UV–visible

analysis was performed in the range of 200–800 nm using a UV-3600 spectrophotometer with a step scan of 2 nm.

2.5. Catalytic reduction of 4-nitrophenol (4-NP)

In a typical experiment, 3 mg of the CuO-NPs catalyst were added to an aqueous solution that contained 4-nitrophenol (25 mL, 2.5 mM,) and freshly prepared aqueous $NaBH_4$ solution (25 mL, 0.25 M). The mixture was stirred at room-temperature. The progress of the catalytic activity, rate of 4-nitrophenol reduction was evaluated by the monitoring of the 4-NP peak at 400 nm employing the UV-visible-NIR spectrophotometer within a range from 250 to 500 nm at RT. The measurement of the apparent rate constant, K was determined by plotting $-\ln(C_t/C_0)$ as a function of time based on pseudo-first order kinetics employing $NaBH_4$ in excess.

The recyclability of the CuO-NPs was estimated for the 3 mg mass sample. The reaction was repeated five times using the same conditions as those used for the fresh catalyst (conditions: 4-NP (2.5 mM), $NaBH_4$ (0.25 M) at room-temperature). The catalyst was separated from the reaction mixture by centrifugation, washed with doubly distilled water and then dried for the next cycle.

To examine the effect of temperature on the reduction of 4-NP via the synthesized catalyst, the reactions were conducted at room temperature (298 K), 308 K, and 318 K.

3. Results and discussion

3.1. XRD analysis

The XRD measurements were done to determine the crystalline nature of the synthesized CuO nanoparticles. The obtained XRD pattern is presented in figure 1. Peaks, at 2θ (°) of 32.5, 35.42, 38.88, 48.79, 56.30, 53.55, 58.29, 61.70, 66.30, 68.20, 72.14 and 75.13 which were assigned to Miller indices (110), (-111), (111), (-202), (020), (202), (113), (022), (022), (220), (311) and (222) planes respectively, were observed. The Peaks resemble a monoclinic structure which is very much in agreement with the standard lattice parameters a = 4.6840 Å, b = 3.4230 Å, c = 5.1290 Å and β=99.54° determined by JCPDS card no. 96–901-4581 [20]. The crystallite size was calculated using the Debye–Scherer's equation:

$$D = \frac{k\lambda}{\beta cos\theta}$$

Where D is the crystallite size, k is a constant = 0.9, λ represents the X-ray wavelength (λ= 1.5406 Å) and β is the Full Width at Half Maximum, FWHM).

The average particle size of CuO-NPs was calculated to be 40 nm by using the above Debye-Scherrer's formula.

3.2.FTIR analysis

The FTIR analysis of the CuO-NPs is shown in figure 2. It was inspected in the presence of biomolecules in peel prickly pear fruits extract that might have been used for the reduction or synthesis of CuO-NPs. The FTIR spectrum of the biologically synthesized CuO-NPs shows the following information bands: the band at 3285 cm^{-1} is associated to the O-H bond of the hydroxyl groups, the band at 2926 cm^{-1} is related to N-H stretching vibrations of the amine group, the band at 1725 cm^{-1} is attributed to the C=O stretching of aldehyde, the bands observed at 1625 cm^{-1} are assigned to cyclic alkene C=C amine stretching vibrations, the band at 1530 is associated to N-O stretching vibrations of the nitro group, the bands at 1222 and 1034 cm^{-1} are due to the C-N bond of the ammine group and to the carboxylic and phenolic groups, respectively. The bands under 1000 cm^{-1} are mainly connected to metal-oxygen bonds. Accordingly, the Cu and O bond appeared at the sharp and intense band of 587 and 426 cm^{-1}. In addition, Cu_2O (Cuprous oxide) bands between 605 and 660 cm^{-1} have not appeared meaning that the phase of the CuO nanoparticles formed are of high purity [21]. The presence of these biologically active plant compounds might have been responsible for the reduction and capping of CuO-NPs. These results were similar to the previous report on the synthesis of CuO-NPs using plant extract [22].

3.3.Optical properties of the CuO nanoparticles

The spectral absorption study of the CuO nanoparticles (dispersed in water) is shown in figure 3. The change of the color from green to dark brown due to the reduction of Copper to CuO nanoparticles in the presence of functional moieties available in prickly pear peel extract. The surface plasmon resonance (SPR) of CuO nanoparticle produced a peak centered near 292 nm in the spectra, which confirmed the formation of CuO nanoparticles which is in agreement with the reported literature [23, 24].

3.4. CuO nanoparticle morphology and elemental analysis

Figure 4(a) shows a SEM image of the synthesized CuO-NPs. The prepared sample shows irregular particles, some of them agglomerated. The SEM images confirmed the size at the nanoscale of the synthesized particles. The Energy dispersive X-ray diffraction spectrum displayed in Figure 4(b). No additional peaks besides the copper and oxygen peaks are noticed, proving the high purity of the synthesized CuO nanoparticles. Atomic percentages of Cu (48.70 %) and O (52.30 %) are measured. Consequently, the weight percentages for Cu (78.88 %) and O (21.12 %) are determined. Additionally, we measured the EDAX mapping, shown in Figure 4(c–d). The blue-colored spots represent the Cu K_α signal whereas the green-colored spots represented the O K_α one. These mappings distinctly manifested the purity of the synthesized

CuO nanoparticles via peel prickly pear fruit extract. The minor signals detected, interpreted as carbon signals because of the biomaterial involved in the CuO-NPs synthesis procedure.

3.5. High-resolution transmission electron microscopy analysis

The TEM study is carried out to understand the crystalline characteristics of the nanoparticles. The shape, size, distribution and crystallinity of the synthesized CuO-NPs were characterized by TEM. The images show spherical NPs, which were quite similar with those observed earlier reports [25, 26]. The size distribution ranges from 20 to 60 nm. The synthesized CuO-NPs exhibit aggregation due to the high surface energy. Black and white regions revealed the hydrophilic and hydrophobic nature of the NPs. The polycrystalline nature matches with the presence of white spots and rings in dark nature [27]. The emerged fringes illustrate the ordered and periodic positioning of the lattice planes in the CuO-NPs (Fig.5 (b)) [28]. Figure 5(c) shows the particle size distribution, being in agreement with the theoretical calculated value form the XRD analysis.

3.6.Catalytic reduction of 4-nitrophenol

The reduction of 4-nitrophenol (NP) to 4-aminophenol (AP) using $NaBH_4$ as a reducing agent has been considered as one of the most popular methods for the reduction of nitro compounds for the determination of the catalytic performance of metal and metal oxide nanoparticles [29]. In agreement with the standard electrochemical potential of 4-NP (E^0(4-NP/4-AP) = 0.76V), and $NaBH_4$ ($E^0(H_3BO_3/BH_4^-)$ = 1.33V), the reduction process is thermodynamically favorable and the reduction can be considered independent of the $NaBH_4$ concentration. As known, the color of 4-NP will change from light yellow to bright yellow after the addition of $NaBH_4$ due to the generation of 4-nitrophenolate when the pH of the solution changes from neutral to alkaline. The unreacted 4-NP exhibits a significant characteristic adsorption band around 400 nm, attributed to the formation of 4-nitrophenolate ions that have a higher π-conjugated donor-acceptor property [30], which is associated with the concentration of 4-NP ions. To evaluate the catalytic activity, the reaction process was examined by monitoring the UV-vis absorption. Figure 6 (a) shows the UV-vis absorption spectra recorded during the reduction of 4-NP catalyzed by CuO-NPs with an interval of 10 min for different temperatures. The intensity of the absorption band drops gradually as the reaction proceeds, accompanied with the appearance of a new absorption peak at 300 nm corresponding to the presence of 4-AP ions [31]. When the catalytic process was over, the mixture solution became colorless. The efficiency $((C_0-C_t)/C_0)$, (C_t and C_0 represent the concentration of 4-NP at time t and the initial concentration of 4-NP, respectively), of 4-NP conversion at different reaction temperatures using the CuO-NPs catalyst

is shown in Figure 6 (b). The conversion rates increased with temperature. The time was fixed to 10 min to determine the conversion efficiency. The reduction efficiency of 4-NP is 96%, 97% and 99% for temperatures of 298 K, 308K and 318K, respectively. Higher temperature ensures a high collision rate of the reactant molecules. Thus, the reduction efficiency of the reaction is increased.

Through the kinetic analysis, the catalytic reduction of 4-NP was a pseudo-first-order reaction, and the kinetic equation was $-\ln\left(\frac{C_t}{C_0}\right) = kt$, where C_t is the concentration of 4-NP at time t, and k is apparent rate constants (Fig.6 (c)). The constant rate was 0.359 min^{-1}, 0.399 min^{-1}, 0.465 min^{-1} for temperatures 298K, 308K, 318K, respectively. The CuO-NPs prepared from prickly pear peel shows higher efficiency compared to similar composite alloy and metal oxide. The variation of Ln(K) vs (1/T) is shown in Figure 6 (d). The activation energy of CuO-NPs was calculated using the Arrhenius equation:

$$ln\ K = \frac{E_a}{RT} + lnA$$

where k is rate of the reaction, A is a constant known as the Arrhenius factor, T is the absolute temperature (Kelvin, K), R is the gas constant (8.3145 $J.mol^{-1}\cdot K^{-1}$) and E_a is the activation energy ($kJ\cdot mol^{-1}$).

Based on the calculation, the activation energy of CuO-NPs is 10.076 $kJ.mol^{-1}$.

The question of the ability of the catalyst to be reused is an important factor in the practical assessment of applications. Therefore, to assess the reuse and stability of the catalyst, CuO-NPs were reused five times at RT (Figure 7). CuO-NPs can be used more than five times after magnetic separation without any loss of catalytic performance of the material. The conversion rate of 4-NP is still close to 93.2% after five successful cycles.

3.7.Mechanism of the reduction of 4-NP

The conceivable mechanism that describes the catalytic performance of the synthesized nanoparticle is described in Figure 8. Copper, like other noble metals, has good electrical conductivity and can rapidly transfer electrons of electron donors adsorbed on its surface to the acceptors, leading to the acceleration of reactions [38]. According to the previously reported catalytic processes of Cu catalyst toward 4-NP [39,40,41], the possible reduction process is depicted in Figure 8(a). $NaBH_4$ was adsorbed and desorbed synchronously on the surface of CuO-NPs, and a copper hydride was also formed at the same time. Subsequently, hydrogen and electrons were transferred to the nitro group of 4-NP, which was converted into 4-AP after hydrogenation [42]. 4-AP was then desorbed from the CuO-NPs and took part in the catalytic reaction again (Figure 8(b)).

4. Conclusion

Copper oxide nanoparticles were synthesized using peel of prickly pear fruit aqueous extract. CuO crystallized in the monoclinic C2/c space group. The refinement of the XRD patterns shows the purity and the high crystalline nature of the synthesized CuO. The FTIR spectra also indicated the presence of the characteristic bands of the vibration modes of the Cu-O bonds and the molecules in fruit extract. SEM images of CuO nanostructure showed agglomerated morphology. The EDX spectra indicate that only peaks corresponding to Cu and O elements are present confirming the pristine nature of CuO nanostructures without any foreign elements prepared through the green synthesis route proposed in this work. The TEM measurements confirmed the nanometric size of the synthesized particles. The reduction of 4-NP to 4-AP was done in 10 min and the efficiency of the reduction increased with temperature. Finally, the examination of the reusable catalyzer led to 93% after five cycles.

References

[1] R. Poreddy, C. Engelbrekt and A. Riisager, Copper oxide as efficient catalyst for oxidative dehydrogenation of alcohols with air, Catal. Sci. Technol. 5 (2015) 2467–2477.

[2] R. Chowdhury, A. Khan, M. H. Rashid, Green synthesis of CuO nanoparticles using Lantana camara flower extract and their potential catalytic activity towards the aza-Michael reaction RSC Adv. 10 (2020) 14374-14385.

[3] J. Singh, V. Kumar, K. H. Kim, M. Rawat, Biogenic synthesis of copper oxide nanoparticles using plant extract and its prodigious potential for photocatalytic degradation of dyes. Environ. Res. 177 (2019) 108569.

[4] K. Kannan, D. Radhika, S. Vijayalakshmi, K. K. Sadasivuni, A. A. Ojiaku, U. Verma, Facile fabrication of CuO nanoparticles via microwave-assisted method: photocatalytic, antimicrobial and anticancer enhancing performance. J. Environ. Anal. Chem. (2020) 1-14.

[5] T. Yu, F. C. Cheong, C. H. Sow, The manipulation and assembly of CuO nanorods with line optical tweezers. Nanotechnology, 15(12) (2004) 1732.

[6] K. R. Reddy, Green synthesis, morphological and optical studies of CuO nanoparticles. J. Mol. Struct. 1150 (2017) 553-557.

[7] M. Ramzan, R. M. Obodo, S. Mukhtar, S. Z. Ilyas, F. Aziz, N. Thovhogi, Green synthesis of copper oxide nanoparticles using Cedrus deodara aqueous extract for antibacterial activity. Mater. Today. 36 (2021) 576-581.

[8] A. C. Nwanya, L. C. Razanamahandry, A. K. H. Bashir, C. O. Ikpo, S. C., Nwanya, S. Botha, M. Maaza, Industrial textile effluent treatment and antibacterial effectiveness of Zea mays L. Dry husk mediated bio-synthesized copper oxide nanoparticles, J. Hazard. Mater. 375 (2019) 281–289.

[9] K. Velsankar, R.M. Aswin Kumar, R. Preethi, V. Muthulakshmi, S. Sudhahar, Green synthesis of CuO nanoparticles via Allium sativum extract and its characterizations on antimicrobial, antioxidant, antilarvicidal activities. J. Environ. Chem. Eng. 8 (2020) 104123.

[10] S. Sun, X. Zhang, Y. Sun, S. Yang, X. Song, Z. Yang, Hierarchical CuO nanoflowers: water-required synthesis and their application in a non-enzymatic glucose biosensor. Phys. Chem. Chem. Phys.15(26) (2013) 10904-10913.

[11] K. Kaviyarasu, G. T Mola, S. O. Oseni, K. Kanimozhi, C. M. Magdalane, J. Kennedy, M. Maaza, ZnO doped single wall carbon nanotube as an active medium for gas sensor and solar absorber. J. Mater. Sc. : Mater. in Elect. 30(1) (2019) 147-158.

[12] J. F. Xu, W. Ji, Z. X. Shen, S. H. Tang, X. R. Ye, D. Z. Jia, X. Q. Xin, Preparation and characterization of CuO nanocrystals. J. Solid State Chem. 147(2) (1999) 516-519.

[13] R. Vijaya Kumar, R. Elgamiel, Y. Diamant, A. Gedanken, J. Norwig, Sonochemical preparation and characterization of nanocrystalline copper oxide embedded in poly (vinyl alcohol) and its effect on crystal growth of copper oxide. Langmuir. 17(5) (2001). 1406-1410.

[14] H. Fan, L. Yang, W. Hua, X. Wu, Z. Wu, S. Xie, B. Zou, Controlled synthesis of monodispersed CuO nanocrystals. Nanotechnology, 15(1) (2003) 37.

[15] Q. Zhang, Y. A. N. Li, D. Xu, Z. Gu, Preparation of silver nanowire arrays in anodic aluminum oxide templates. J. Mater. Sci. Lett 20(10) (2001) 925-927.

[16] R. Palmeri, L. Parafati, E. Arena, E. Grassenio, C. Restuccia, B. Fallico, Antioxidant and antimicrobial properties of semi-processed frozen prickly pear juice as affected by cultivar and harvest time. Foods, 9(2) (2020) 235.

[17] E.B. Hossam, M. Heba, E. Aya, E. Sara, S. Gehan. Phytochemical screening, antimicrobial, antiaxidant, anticancer activities and nutritional values of cactus (opuntia ficus indicia) pulp and peel. Fresenius Environ. Bull. 28 (2019) 1534-1551.

[18] M. Kamaraj, T. G. Nithya, P. Chidambararajan, M. Kebede, Photocatalytic degradation of Bisphenol-A in water under sunlight irradiation over ZnO nanoparticles fabricated by Ethiopian cactus pear fruit peel infusions. Optik, 208 (2020) 164539.

[19] M. G. Muñoz-Carrillo, C. Garcidueñas-Piña, R. C. Valerio-García, J. L. Carrazco-Rosales, J. F. Morales-Domínguez, . Green Synthesis of Silver Nanoparticles from the Opuntia ficus-indica Fruit and Its Activity against Treated Wastewater Microorganisms. J. Nanomater. (2020).

[20] S. Asbrink, L. J. Norrby, A refinement of the crystal structure of copper (II) oxide with a discussion of some exceptional esd's. Acta Cryst. Section B 26 (1970) 8-15.

[21] R. Sankar, P. Manikandan, V. Malarvizhi, T. Fathima, K.S. Shivashangari, V. Ravikumar, Green synthesis of colloidal copper oxide nanoparticles using Carica papaya and its application in photocatalytic dye degradation, Spectrochim. Acta A Mol. Biomol. Spectrosc. 121 (2014) 746–750.

[22] S. Saif, A. Tahir, T. Asim, Y. Chen, Plant mediated green synthesis of CuO nanoparticles: comparison of toxicity of engineered and plant mediated CuO nanoparticles towards Daphnia magna, Nano. 6 (2016) 205.

[23] M. Rafique, F. Shafiq, S. S. A.Gillani, M. Shakil, M. B.Tahir, I. Sadaf, Eco-friendly green and biosynthesis of copper oxide nanoparticles using Citrofortunella microcarpa leaves extract for efficient photocatalytic degradation of Rhodamin B dye form textile wastewater. Optik, 208 (2020) 164053.

[24] P. Yugandhar, T. Vasavi, P. U. M. Devi, N. Savithramma, Bioinspired green synthesis of copper oxide nanoparticles from Syzygium alternifolium (Wt.) Walp: characterization and evaluation of its synergistic antimicrobial and anticancer activity. Appl. Nanosci. 7(7) (2017) 417-427.

[25] S. Meghana, P. Kabra, S. Chakraborty, N. Padmavathy, Understanding the pathway of antibacterial activity of copper oxide nanoparticles, RSC Adv. 5 (16) (2015)12293–12299.

[26] Nagar, N., & Devra, V. Green synthesis and characterization of copper nanoparticles using Azadirachta indica leaves. Mater. Chem. and Phys. 213 (2018) 44-51.

[27] K. Velsankar, S. Sudhahar, G. Parvathy, R. Kaliammal, Effect of cytotoxicity and Antibacterial activity of biosynthesis of ZnO hexagonal shaped nanoparticles by Echinochloa frumentacea grains extract as a reducing agent, Mater. Chem. Phys. 239 (2020) 121976.

[28] Z.U.H. Khan, H.M. Sadiq, N.S. Shah, A.U. Khan, N. Muhammad, S.U. Hassan, K. Tahir, S.Z. Shafi, F.U. Khan, M. Imran, N. Ahmad, F. Ullah, A. Ahmad, M. Syed, M.S. Khalid, S.A. Qaisrani, M. Ali, M.Z. Ali, Greener synthesis of zinc oxide nanoparticles using Trianthema portulacastrum extract and evaluation of its photo-catalytic and biological applications, J. Photochem. Photobiol. 192 (2019) 147–157.

[29] K. Kuroda, T. Ishida and M. Haruta, Reduction of 4-nitrophenol to 4-aminophenol over Au nanoparticles deposited on PMMA. J. Mol. Catal. A: Chem., 298 (2009) 7–11.

[30] R. Das, V.S. Sypu, H.K. Paumo, M. Bhaumik, V. Maharaj, A. Maity, Silver decorated magnetic nanocomposite (Fe_3O_4@PPy-MAA/Ag) as highly active catalyst towards reduction of 4-nitrophenol and toxic organic dyes, Appl. Catal. B Environ. 244 (2019) 546–558.

[31] T. Premkumar, K. Lee, K.E. Geckeler, Shape-tailoring and catalytic function of anisotropic gold nanostructures, Nanoscale Res. Lett. 6 (2011) 1–12.

[32] L. Zhi, H. Liu, Y. Xu, D. Hu, X. Yao, J. Liu, Pyrolysis of metal–organic framework (CuBTC) decorated filter paper as a low-cost and highly active catalyst for the reduction of 4-nitrophenol, Dalton Trans. 47 (2018) 15458–15464.

[33] C. Chu, S. Rao, Z. Ma, H. Han, Copper and cobalt nanoparticles doped nitrogen-containing carbon frameworks derived from CuO-encapsulated ZIF-67 as high-efficiency catalyst for hydrogenation of 4-nitrophenol, Appl. Catal. B Environ. 256 (2019), 117792.

[34] N.E. Larm, J.A. Thon, Y. Vazmitsel, J.L. Atwood, G.A. Baker, Borohydride stabilized gold–silver bimetallic nanocatalysts for highly efficient 4-nitrophenol reduction, Nanoscale Adv. 1(12) (2019).

[35] J. Nimita Jebaranjitham, C. Mageshwari, R. Saravanan, N. Mu, Fabrication of amine functionalized graphene oxide-AgNPs nanocomposite with improved dispersibility for reduction of 4-nitrophenol, Compos. Part B Eng. 171 (2019) 302–309.

[36] X. Zhang, N. Wang, L. Geng, J. Fu, H. Hu, D. Zhang, et al., Facile synthesis of ultrafine cobalt oxides embedded into N-doped carbon with superior activity in hydrogenation of 4-nitrophenol, J. Colloid Interface Sci. 512 (2018) 844–852.

[37] B. Xu, X. Li, Z. Chen, T. Zhang, C. Li, Pd@MIL-100(Fe) composite nanoparticles as efficient catalyst for reduction of 2/3/4-nitrophenol: synergistic effect between Pd and MIL-100(Fe), Microporous Mesoporous Mater. 255 (2018) 1–6.

[38] A. Bhattacharjee, M. Ahmaruzzaman, Green synthesis of 2D CuO nanoleaves (NLs) and its application for the reduction of p-nitrophenol. Mater. Lett. 161 (2015) 79-82.
[39] X. Kong, H. Zhu, C. Chen, G. Huang, Q. Chen, Insights into the reduction of 4-nitrophenol to 4-aminophenol on catalysts. Chem. Phys. Lett. 684 (2017) 148-152.

[40] D. Ayodhya, G. Veerabhadram, Influence of g-C_3N_4 and g-C_3N_4 nanosheets supported CuS coupled system with effect of pH on the catalytic activity of 4-NP reduction using $NaBH_4$. Flat Chem. 14 (2019) 100088.

[41] A. A. Kassem, H. N. Abdelhamid, D. M. Fouad, S. A. Ibrahim, Metal-organic frameworks (MOFs) and MOFs-derived CuO@C for hydrogen generation from sodium borohydride. Int. J. Hydrog. Energy. 44(59) (2019) 31230-31238.

[42] G. Marcelo, A. Muñoz-Bonilla, M. Fernández-García, Magnetite–polypeptide hybrid materials decorated with gold nanoparticles: study of their catalytic activity in 4-nitrophenol reduction. J. Phys. Chem. C 46 (2012) 24717-24725.

Figure 1. X-ray diffraction pattern and unit cell (inset) of the synthesized copper oxide nanoparticles.

Figure 2: The FTIR spectra of synthesized copper oxide nanoparticles.

Figure 3: UV-visible absorption spectrum of the as-synthesized copper oxide nanoparticles.

Figure 4 : (a) SEM image of the CuO-NPs, (b) EDX pattern and the corresponding elemental maps of (c) Cu and (d) O in the CuO-NPs.

Figure 5: (a) TEM images **(b)** magnification showing the lattice planes **(c)** grain size distribution of the CuO-NPs.

Figure 6: **(a)** Time-dependent UV−vis spectra of 4-NP reduction catalyzed by as green synthesized CuO-NPs as a catalyst at different temperatures, **(b)** plots of 4-NP reduction efficiency catalyzed by CuO-NPs at different temperatures, **(c)** kinetic analysis of 4-NP reduction catalyzed by CuO-NPs at different temperatures and **(d)** variation of Ln(*K*) vs (1/T).

Figure 7: Cycling performance of CuO-NPs in the catalytic reduction of 4-NP.

Figure 8: (a) Schematic illustration of 4-nitrophenol reduction by $NaBH_4$ catalyzed by CuO-NPs. **(b)** the mechanism for the reduction of 4-nitrophenol to 4-aminophenol.

Figure 1

Click here to access/download;Figure;Figure 1.docx

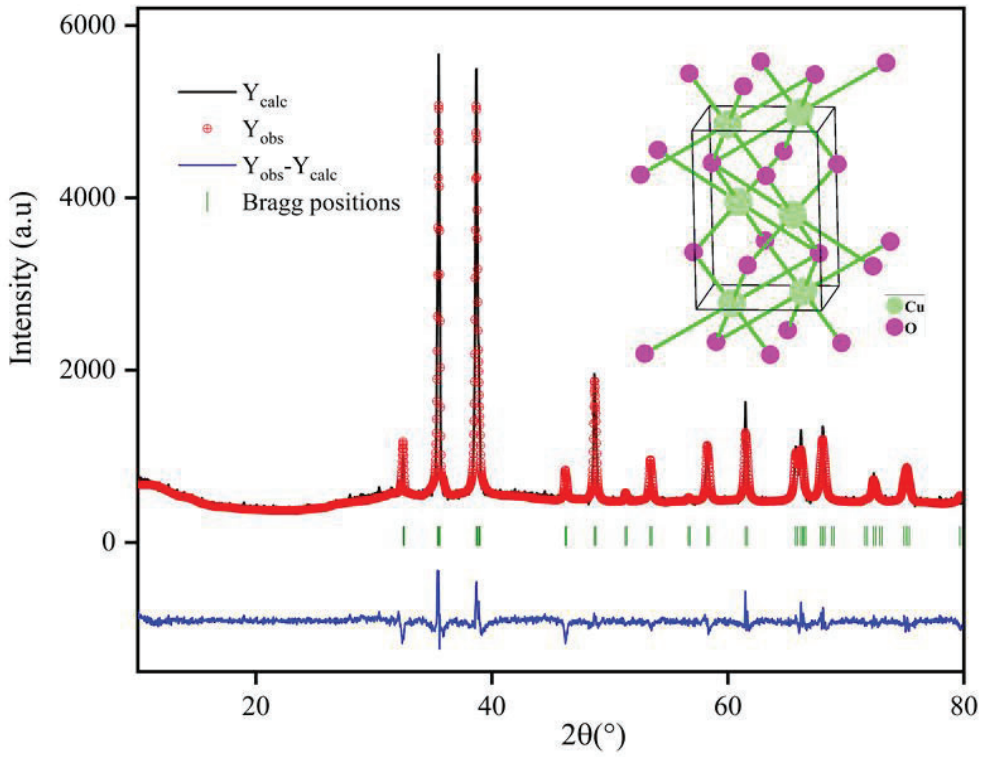

Figure 2

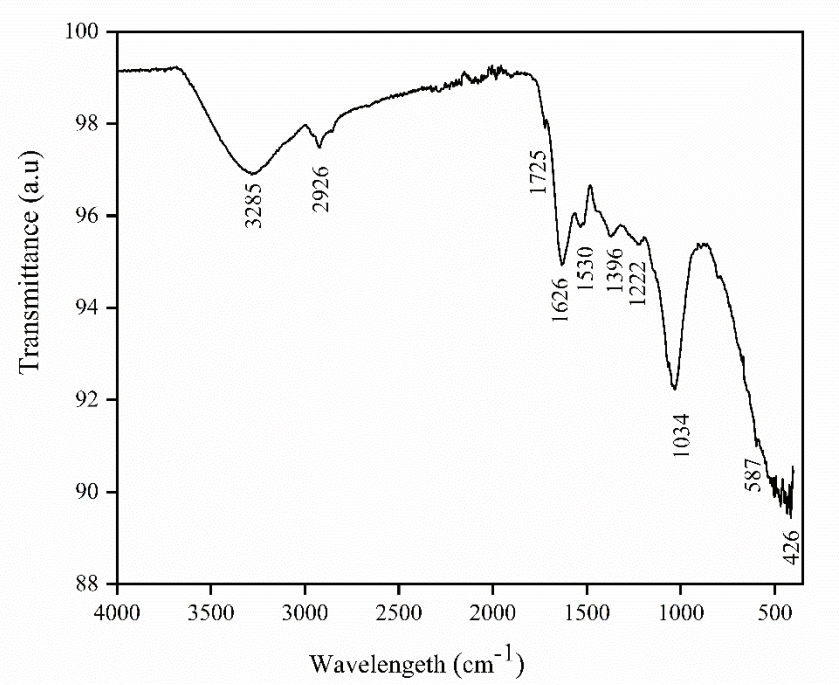

Figure 3

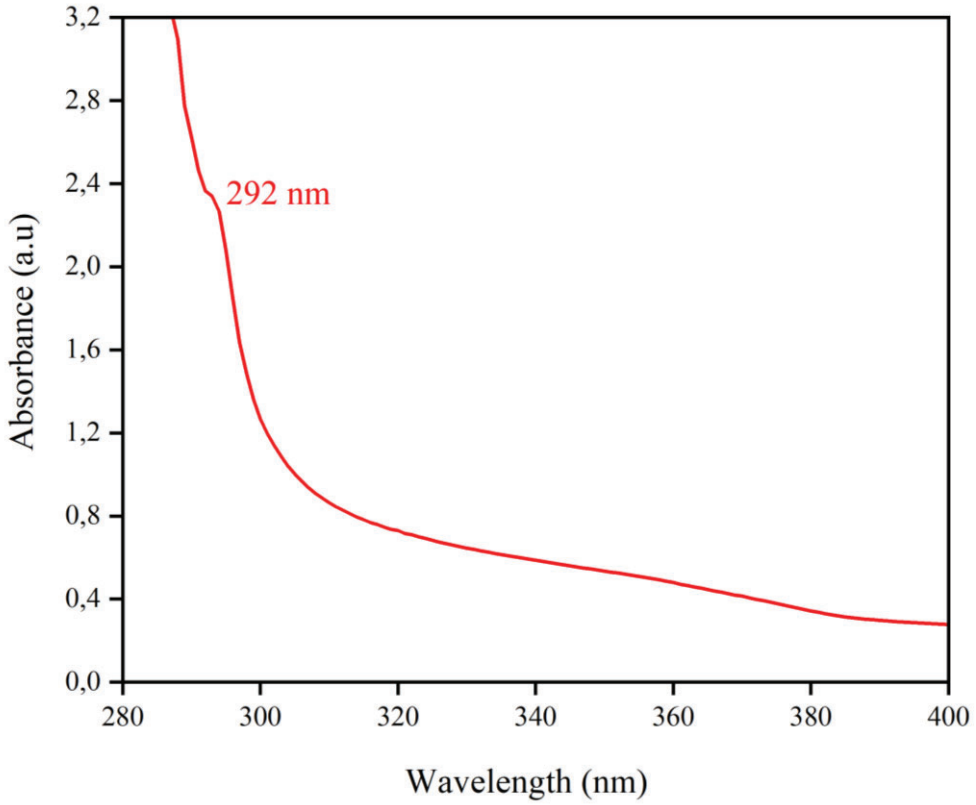

Figure 4

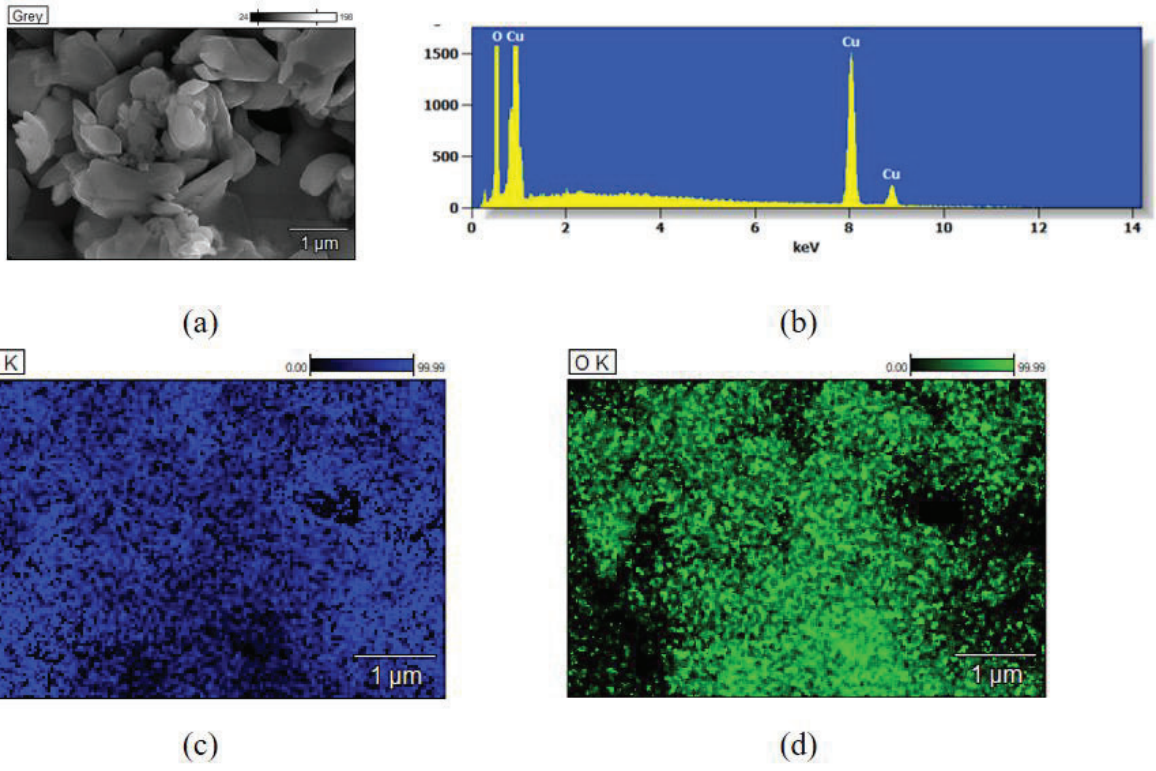

Figure 5

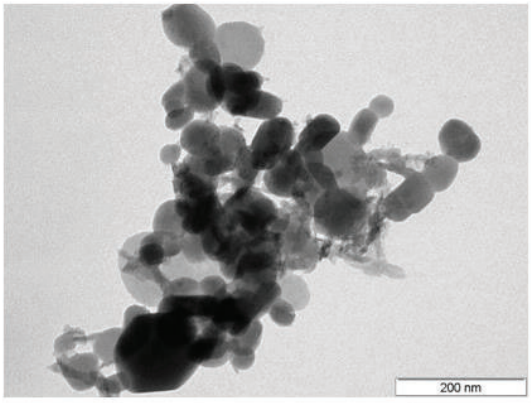

(a)

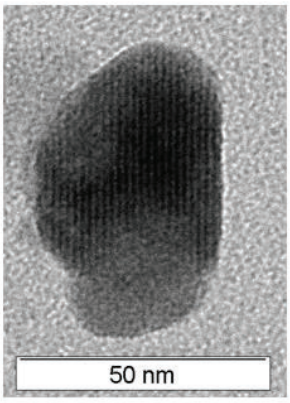

(b)

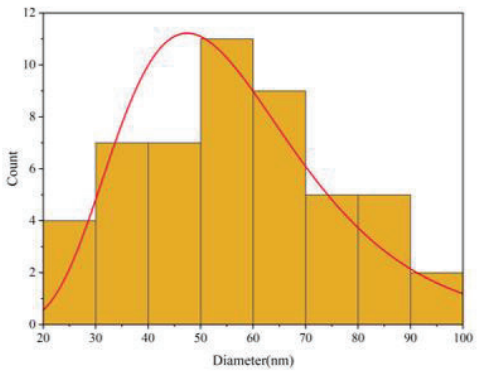

(c)

Figure 6

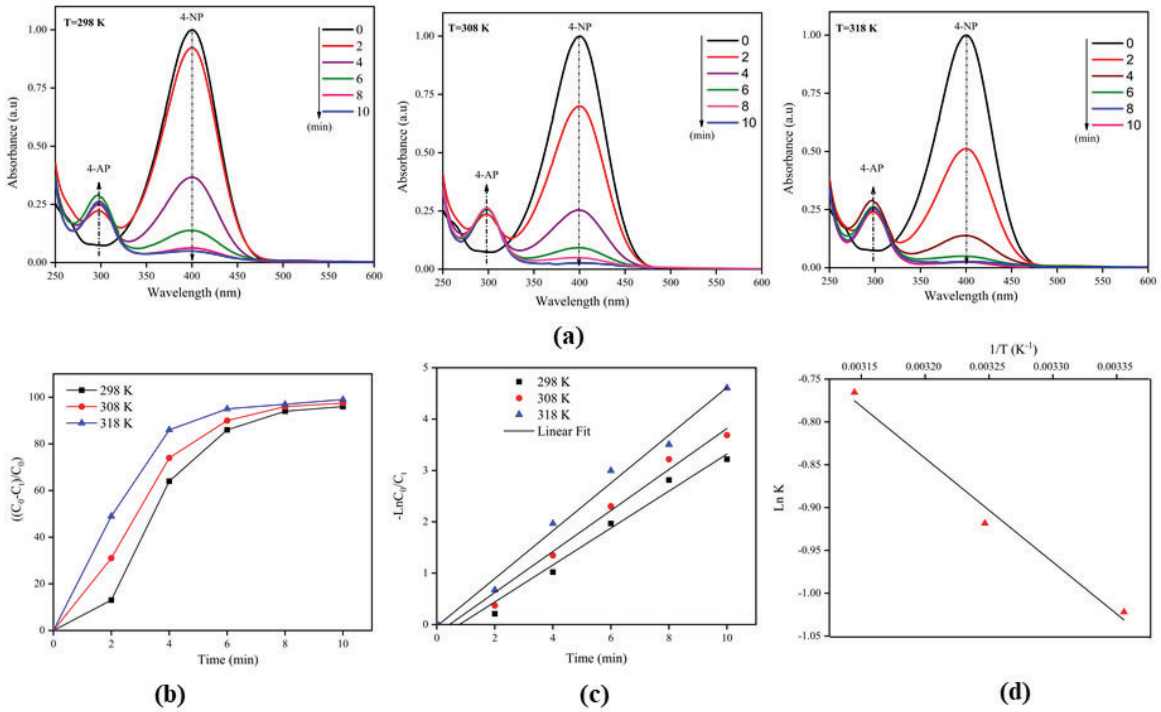

(a)

(b)

(c)

(d)

Figure 7

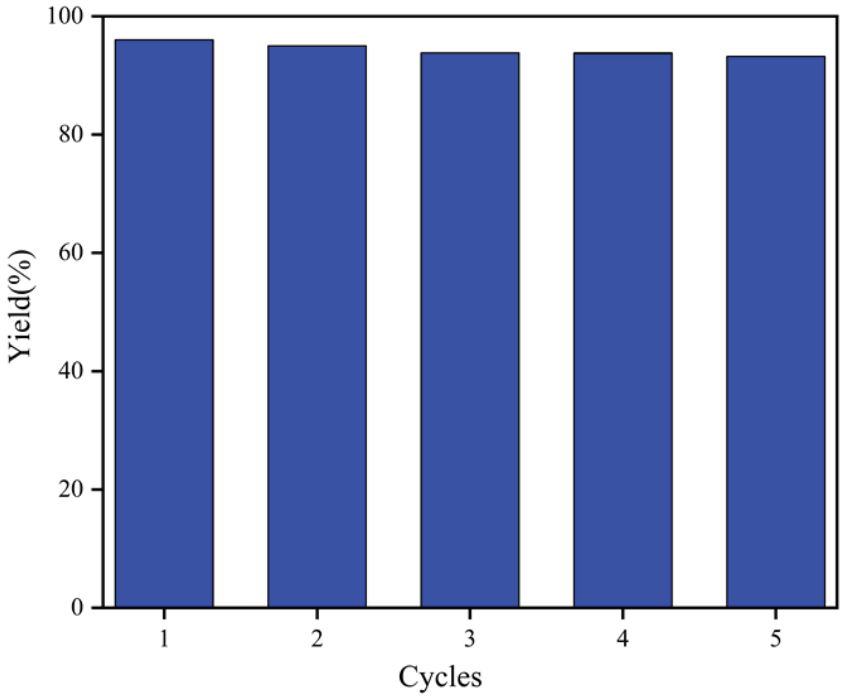

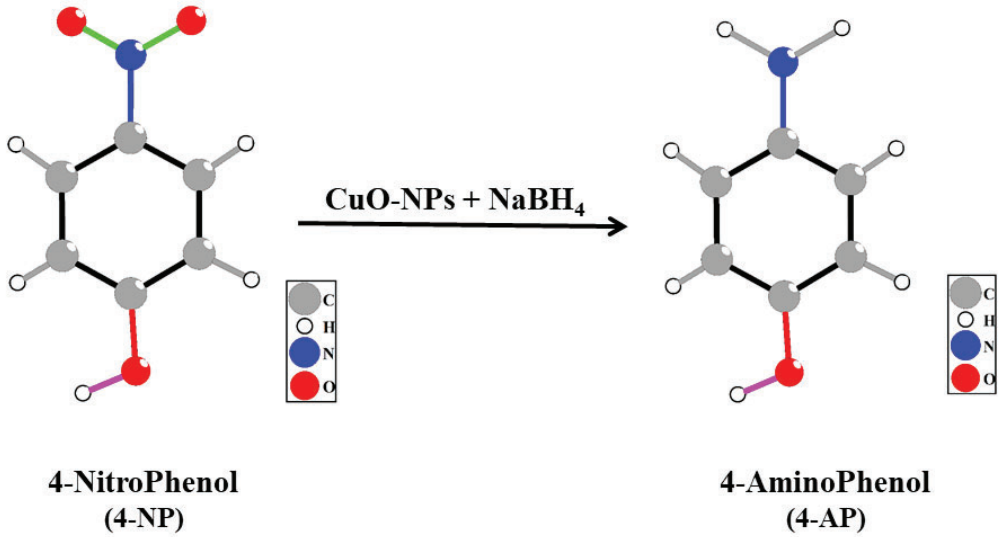

(a)

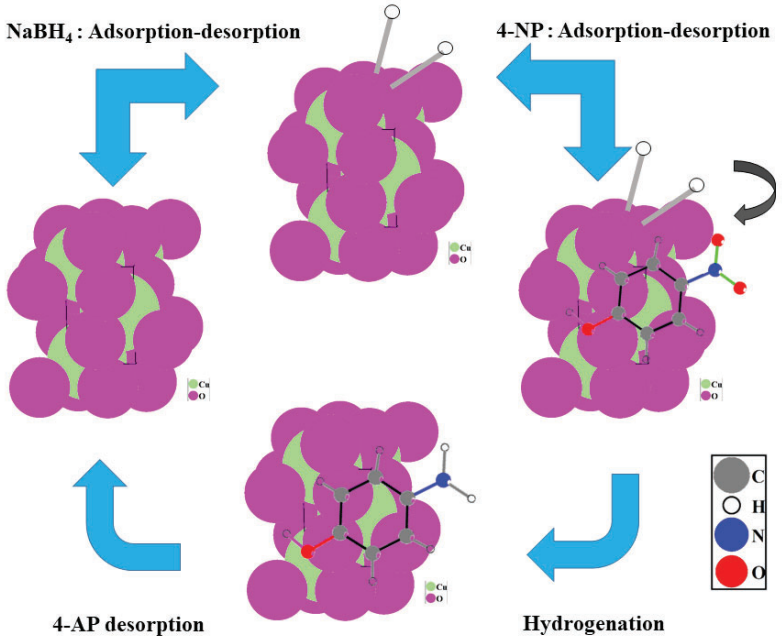

(b)

Table 1: Comparative study of 4-NP reduction in the presence of $NaBH_4$ as a reducing agent with various catalysts.

Catalysts	Conditions	Conversion (%)	Rate (s^{-1})	Ref.
Cu_xO@C	Cat. (2 mg), 4-NP (16 µmol), $NaBH_4$ (1 mol)	-	4.8×10^{-3}	32
Cu/Co@NCF	Cat. (10 mg mL^{-1}), 4-NP (0.3 µmol), $NaBH_4$ (0.6 mmol)	-	69.3×10^{-3}	33
Au_xAg_{1-x}	Cat. (0.2 mM), 4-NP (0.1 M), $NaBH_4$ (0.25 mM)	95	1.9×10^{-1}	34
Ag@GO	Cat. (1 mg), 4-NP (0.1 mM), $NaBH_4$ (100 mM)	100	7.5×10^{-4}	35
CoO_x/CN	Cat. (2 mg), $NaBH_4$ (10 mmol), 4-NP (8 mmol)	95	4.2×10^{-3}	36
Pd@MIL-100	Cat. (0.525 mg), $NaBH_4$ (54 mg), 4-NP (94 mg/L)	-	6.5×10^{-3}	37
CuO	Cat. (3.0 mg)), $NaBH_4$ (0.3M), 4-NP (0.2mM)	96	$5,9\ 10^{-3}$	This work

NCF: nitrogen-containing carbon frameworks

GO: graphene oxide

CN : N-doped carbon